A Novel Waveform-Tracking BLE Receiver

Suoping Hu, *Member, IEEE,* Peng Chen, *Member, IEEE,* Philip Quinlan, *Member, IEEE,* and Robert Bogdan Staszewski, *Fellow, IEEE*

***Abstract*—We present a first-ever waveform-tracking receiver (RX) with type-II phase-tracking loop. In this preprint, a novel nonlinear filter in the feedback path is proposed to obtain better interference rejection performance. This digital nonlinear filter assists the receiver with tracking the waveform intelligently by predicting the incoming symbols; hence, we define this proposed RX as a waveform-tracking (WT)-RX. The simulation and preliminary measurement results are demonstrated in this paper. Moreover, we explore the issues of the current version WT-RX to provide guidance on possible future follow-up activities.**

***Index Terms*—Bluetooth low energy (BLE), digitally controlled oscillator (DCO)-based receivers (RXs), discrete-time (DT) filter, discrete-time (DT) receivers, Internet-of-Things (IoT), waveform-tracking RXs (WT-RXs), successive-approximation-register (SAR)-analog-to-digital converter (ADC), ultra-low power (ULP), ultra-low voltage (ULV).**

I. Introduction

TO meet the increasing amount of Internet-of-Things (IoT) nodes, the wireless RXs must meet the requirements of high power efficiency and selectivity. BLE requires at least 17/27-dB of interferer rejection at 2/3-MHz offsets. Due to operating in the crowded 2.4-GHz ISM band, the BLE RXs are expected to face more stringent specifications for the next-generation IoT nodes. The phase-tracking receivers [1], [2], [3], [4] have been proven superior in energy efficiency, while their selectivity is severely restricted from further improving by the loop delay as a result of the required sharp filtering. Despite the fact that our previous work in [2], [3] meet the BLE specs with a 2∼3-dB margin, they compromise the selectivity compared to the conventional open-loop Cartesian RXs, where the interference rejection ratio is only limited by the filter bandwidth as long as the RX is not saturated. A >10-dB specification margin can be easily obtained with a high-order sharp filtering [5], [6] and optimization on the linearity of subblocks [7], [8]. However, this requires at least 2× the power and area of the PT-RX due to the I/Q demodulation.

Staszewski *et al.* [9] have proposed and demonstrated an interpolative GFSK pulse-shape filtering for wireless RF transmitters with an arbitrary reference frequency. Inspired by that work, we propose an efficient nonlinear pulse-shape filtering for the WT-RX to improve the signal-to-noise ratio (SNR) of the oscillator tuning word (OTW). Based on the stored previous two symbols, this WT-RX predicts the ongoing GFSK symbol and makes the decision "intelligently".

Manuscript received 11th, March, 2022. This work was supported in part by the Science Foundation Ireland under Grant 14/RP/I2921, and in part by Analog Devices, Cork, Ireland.

Suoping Hu, Peng Chen, Robert Bogdan Staszewski are with the School of Electrical and Electronic Engineering, University College Dublin, Dublin 4, D04 V1W8, Ireland (e-mail: suoping.hu@ucdconnect.ie).

Philip Quinlan is with Integrated Networking Products, Analog Devices, Cork, T12 X36X, Ireland. (e-mail: Philip.Quinlan@analog.com)

II. Proposed Waveform-Tracking RX

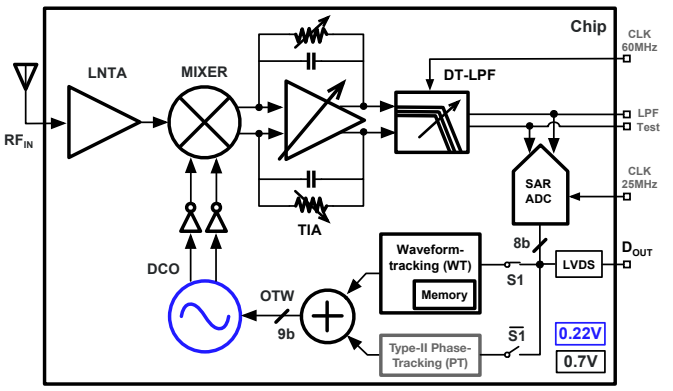

Fig. 1. Simplified diagram of the proposed WT-RX.

Figure 1 shows a simplified diagram of the proposed WT-RX, which is identical to the one shown in [2][1]. The digitally controlled oscillator (DCO) tracks the RF input, and the passive mixer detects the residual frequency difference between them. The discrete-time LPF would filter out undesired components, i.e., interferers, high-order harmonics, etc, after the transimpedance amplifier (TIA). A low-power SAR ADC is utilized to digitize the phase difference between RF input and DCO output signal. To verify the effectiveness of the waveform-tracking loop, a test-mode multiplexer is applied to select either the phase-tracking or waveform-tracking operation.

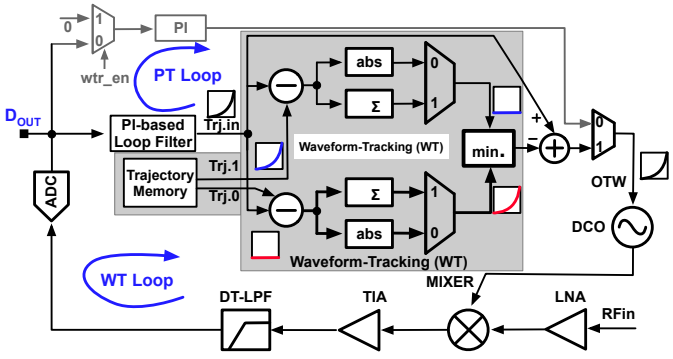

Fig. 2. Proposed RX emphasizing the details of the nonlinear waveform-tracking filter.

A. Proposed Non-linear Waveform-Tracking Filter

Figure 2 illustrates the proposed waveform-tracking loop in detail. The detected trajectory from the ADC is fed into the

[1]Note: switch S1 is now turned on.

PI-based loop filter. Subtracting the two pre-stored reference candidates (i.e., "Trj.1" and "Trj.0") in the trajectory memory block from the PI controller's output (see "Trj.in" in Fig. 2), we can obtain two candidates of the residual error. The multiplexer is used to select either the integrated or absolute value of the residual error candidates, depending on the investigation objectives. The trajectory candidate with the minimum residual error is picked and then delivered as the OTW of the DCO. The trajectory memory, together with the waveform-tracking block, functions as a nonlinear waveform-tracking filter.

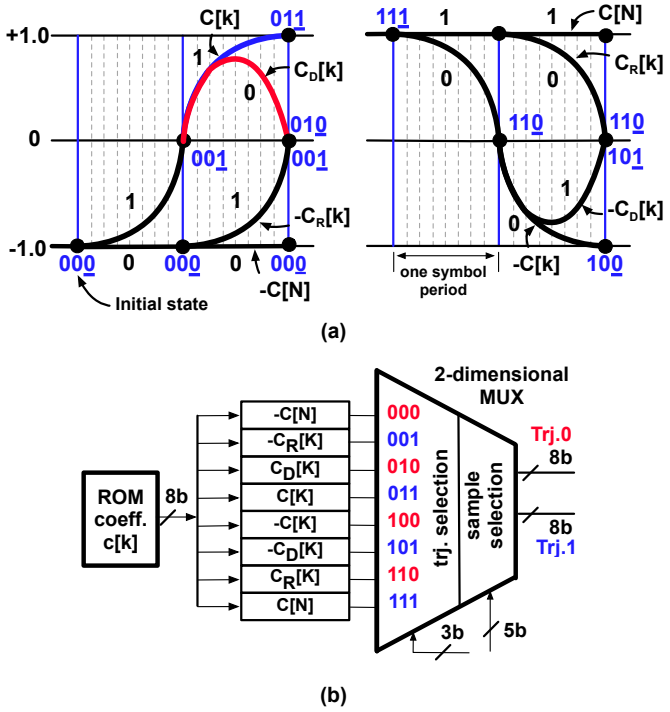

Fig. 3. (a) Trajectories for various state transitions based on previous symbol values. (b) Implementation of the trajectory memory block.

The implementation of the trajectory memory block is illustrated in Fig. 3. It stores all eight possible states (i.e., trajectories) from the combination of three binary symbols (the current and previous two symbols), such as the red curve "010", as shown in Fig. 3(a). In Fig. 3(a), each symbol (1 μs period) is 8$\times$ oversampled[2] and waveform-tracking block makes a decision every sampling cycle to minimize the risk of incorrect tracking. The blue vertical line refers to the last sample of a state where the WT block updates the right-hand bit and enters to the tracking period for the next symbol. Let us make an example to gain an in-depth insight. Assume that the previous two states are known as "01", for the first few samples, both candidates "Trj.1" [see the blue curve in Fig. 3(a)] and "Trj.0" [see the red curve in Fig. 3(a)] are identical. However, after a half period (0.5 μs) the difference between the two candidates keeps growing, which indicates the waveform-tracking block has a better odds to make a correct decision at the latter half period of the symbol. If the detected trajectory from the loop filter is "011" (where the right-hand

[2]To simply the analysis, Fig. 3(a) only demonstrates an 8$\times$ oversampling, but in this work we have implement a 25$\times$ oversampling.

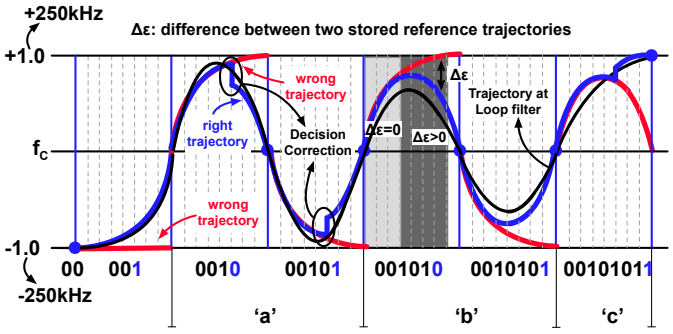

Fig. 4. Conceptual illustration of waveform-tracking (WT) non-linear filter.

bit is the most recent one), the blue curve in Fig. 3(a) is the correct candidate and the red one (referring to "010") is wrong.

All coefficients of the remaining trajectories can be derived from the fundamental $C[k]$ (see equation 1), which forms the trajectory "011".

$$C[k] = \sum_{n=0}^{k-1} h[n] \tag{1}$$

where $h[n]$ is the impulse response of the Gaussian filter in discrete-time domain and can be derived with a fixed modulation index m, e.g., $m = 0.5$ for BLE, as stated in [9]. $C[k]$ is pre-calculated and stored in a look-up table with $k = 0, ..., N-1$ being the index. N is the oversampling ratio (OSR), which is 25 in this work. $C_R[k]$ represents the reversed-order coefficients, which are computed as

$$C_R[k] = C[N-k] \tag{2}$$

where $C[N]$ is the maximum value of the accumulated coefficient, e.g., $+1.0$. The di-bit coefficients $C_D[k]$ are computed as

$$C_D[k] = C[k] + C[N-k] - C[N-1] \tag{3}$$

To save the hardware cost, only $C[k]$ coefficients are pre-stored in a read-only memory (ROM)-like fashion, and the rest are pre-calculated on power-up through an arithmetic combinatorial logic. A two-dimensional multiplexer is used in Fig. 3(b) to select the 3-bit trajectory and 5-bit sample, respectively.

Figure 4 conceptually illustrates an example of processing the waveform tracking with an input symbol sequence of "00101011". The black curve refers to the detected trajectory from the loop filter, and the blue one is the recovered correct trajectory. Due to the non-ideality of the tracking loop, such as gain error, the detected trajectory could be different from the GFSK waveform. In the case of 'a', "Trj.in" exhibits a slight overshoot (i.e., overestimated gain) and a sudden jump happens at the fifth sample, where the decision is corrected. Meanwhile, an underestimated gain could cause a dumped "Trj.in", which is not an issue when the current input symbol is "0", such as the case of 'b', but it results in the sudden jump in the case of symbol "1", as shown in the case of 'c'. This jump or glitch could be minimized by reducing the decision-making interval, such as every sample.

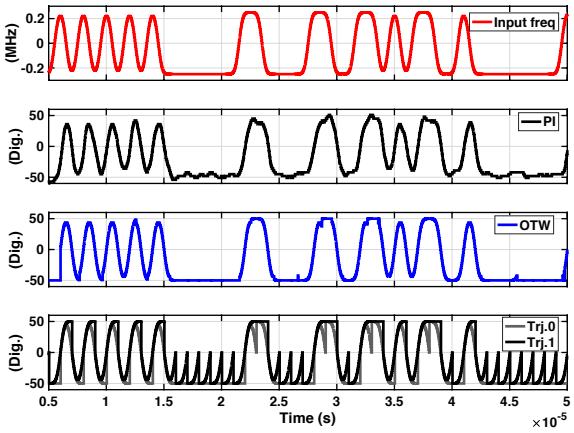

Fig. 5. Simulated output waveforms of PI and OTW with −67 dBm RF input.

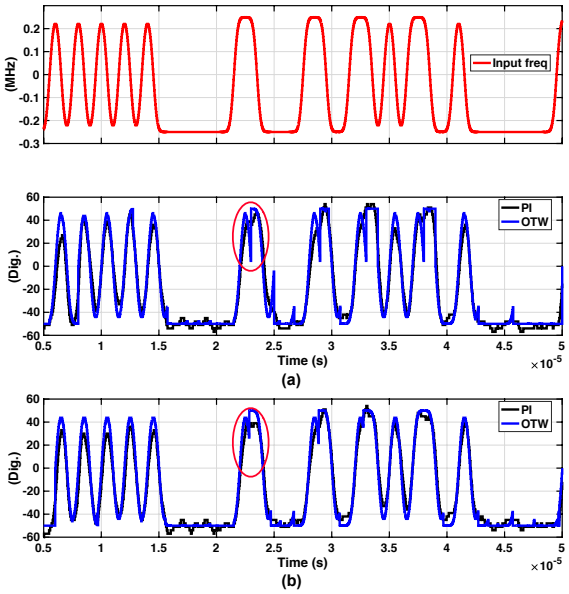

Fig. 6. Simulated output waveforms of PI and OTW with various decision-making rates: (a) every eight samples, (b) every sample.

B. Simulation Results

A behavioral model is built in Simulink to verify the effectiveness of the proposed WT-RX[3]. The simulated output waveforms of PI and OTW are demonstrated in Fig. 5. It is clear that the OTW trajectory demonstrates a nearly perfect recovery of the input GFSK-modulated data sequences and is much smoother than the detected one from the PI controller, which verifies the effectiveness of the proposed WT-RX. Note that the tiny "jump" of OTW output in Fig. 5 is because of the wrong initial prediction of the next symbol, which can be reduced by increasing the sampling frequency. The trajectories of the two reference candidates are also shown. Since the loop gain has been set to match with the input frequency range, the

[3]RX NF = 8 dB; 1 dB compression point of RX, CP_{1dB} = 0 dBm; phase noise (PN) of DCO = −112 dBc/Hz at 1 MHz offset; and RF input is −67 dBm.

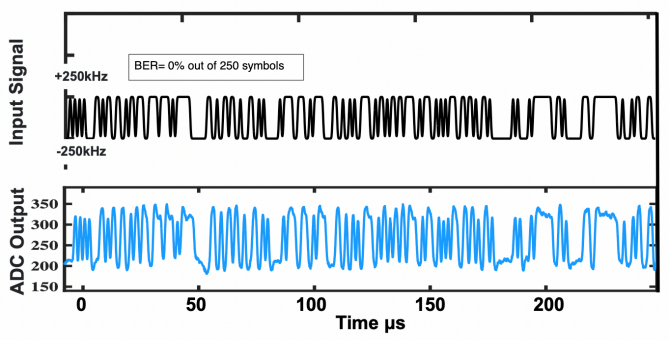

Fig. 7. The recovered output of ADC with a RF input level of −67 dBm and GFSK modulated symbols.

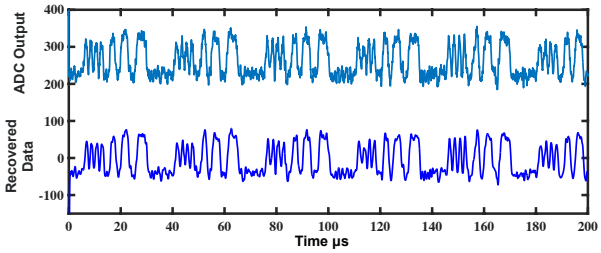

Fig. 8. The recovered output of ADC with a RF input level of −84 dBm and GFSK modulated symbols.

"jump" mentioned in Section II-A is minimized. The simulated output waveforms with 25% larger loop gain are shown in Fig. 6, where the "jump" is much worse than the case with normal loop gain. Besides, a large interval (i.e., 8 samples) between each comparison decision could cause a spur or even a tracking error, as shown in Fig. 6(a), thus a small interval between each comparison decision (i.e., 1 sample) is preferred. Figure 6(b) shows that the spur level is reduced dramatically by applying one-sample-based decision-making.

III. Experimental Results

A. Preliminary Results

Figure 7 plots the ADC output of a GFSK-modulated pseudorandom data with −67-dBm at the RF input. Figure 8 shows the ADC output with a GFSK-modulated regular data pattern ("10101010000111...") and the RF input power of −84 dBm. The recovered data is obtained by applying a post-processing filter, which is a moving average filter with a window size of up to 14 samples. These two figures indicate that the waveform-tracking loop works properly. However, due to some bugs and issues of the current version, we cannot obtain further performance results in terms of ACR and sensitivity, which will be discussed in the following section.

B. Bugs in the Current Version WT-RX

This section discloses several "bugs" of the current version of WT-RX, such as gain normalization for the reference trajectories, overflow of the detected trajectory difference, and data pattern constraints.

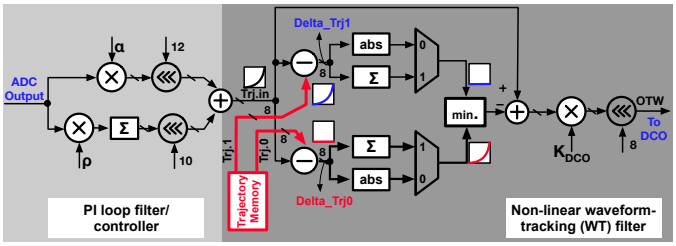

Fig. 9. The non-linear waveform-tracking filter implementation in detail.

1) Gain Normalization Issue: The first recognized issue from the measurements is the lack of gain normalization for the reference trajectories in the ROM block. To minimize the decision-making error, the output range of the reference trajectories ("Trj.1" and "Trj.0" in Fig. 9) must be adapted to match with the detected trajectories from the PI controller ("Trj.in" in Fig. 9). However, in this version, the trajectory memory block (see Fig. 9) is implemented with a fixed 8-bit range without any programmablity. Note that with some specific input level, analog gain, and PI coefficients, the RX can still demodulate successfully; however, it does not allow us to change the input signal level.

Fig. 10. Waveforms at various nodes with (a), and without (b) the overflow issue.

2) Overflow Issue: Another issue is the overflow of the 8-bit register [nodes "Delta_Trj0" and "Delta_Trj1" in Fig. 9] storing the difference between the detected and pre-stored trajectory. There are several scenarios where this overflow would happen: 1) "Trj.in" could exceed the 8-bit range due to a severe interference disturbance; 2) the detected trajectory "Trj.in" is corresponding to symbol "1" while the reference trajectory is delivering symbol "0"; namely, the difference between these two trajectories is maximized due to a wrong decision. Figure 10(a) plots the waveforms of various output nodes (e.g., LPF, PI, OTW) when the overflow happens, which results in consecutive errors. Figure 10(b) shows the case where the overflow bug is solved by merely doubling the range of the related registers. This indicates that to fix this overflow bug in all scenarios, the simplest and most effective way would be adding enough redundancy to the corresponding registers.

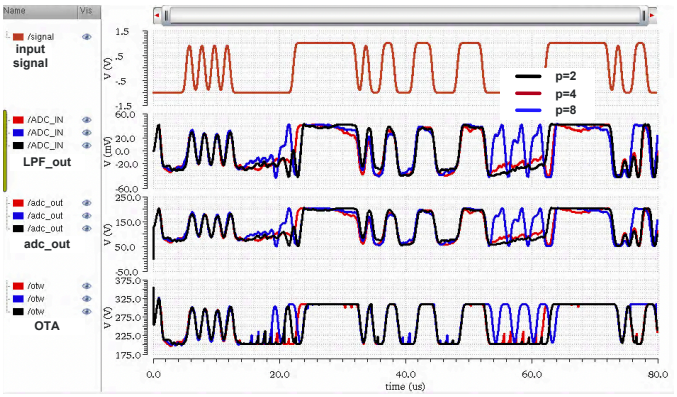

Fig. 11. The waveforms at various nodes with different values of integral coefficient ρ.

3) Data Pattern Constraint: Lastly, similar to the type-I PT-RX, the digital integrator in the non-linear waveform-tracking loop does not function effectively to zero out the residual phase error. This indicates that the consecutive symbols, i.e., "1" or "0", could fail the tracking loop eventually. The digital integrator could accelerate this failure process due to this nonzero phase error [2]. Figure 11 plots the waveforms at various nodes, such as LPF output, ADC output, and DCO input (OTW), with different values of the integral coefficient ρ.

IV. Conclusion

A waveform-tracking receiver is proposed in this paper to further suppress the adjacent channel interference in a non-linear manner. As a highly experimental prototype, although it suffers from some "bugs" and issues, which restrict its performance, the preliminary measured results suggest that the basic functionality of waveform-tracking works properly. In addition, the proposed WT-RX achieves a 2-dB improvement in terms of ACR at 2 MHz offset per simulations. Therefore, it provides a possibility of mitigating the trade-off between loop delay and interference rejection in the PT-RXs with a more sophisticated digital signal processing.

References

[1] M. Ding, X. Wang, P. Zhang, Y. He, S. Traferro, K. Shibata, M. Song, H. Korpela, K. Ueda, Y.-H. Liu *et al.*, "A 0.8-V 0.8 mm^2 bluetooth 5/BLE digital-intensive transceiver with a 2.3-mW phase-tracking RX utilizing a hybrid loop filter for interference resilience in 40nm CMOS," in *2018 IEEE International Solid-State Circuits Conference-(ISSCC)*. IEEE, 2018, pp. 446–448.

[2] S. Hu, J. Du, P. Chen, H. M. Nguyen, P. Quinlan, T. Siriburanon, and R. B. Staszewski, "A Type-II Phase-Tracking Receiver," *IEEE Journal of Solid-State Circuits*, vol. 56, no. 2, pp. 427–439, 2021.

[3] S. Hu, P. Chen, P. Quinlan, and R. B. Staszewski, "A 0.7-V Sub-mW Type-II Phase-Tracking Bluetooth Low Energy Receiver in 28-nm CMOS," *IEEE Transactions on Circuits and Systems I: Regular Papers*, vol. 68, no. 6, pp. 2317–2328, 2021.

[4] S. Hu, "Ultra-Low-Power Phase-Tracking Receivers for IoT Applications," Ph.D. dissertation, Elect. Electron. Eng., Univ. College Dublin, Dublin, Ireland, 2021. [Online] http://hdl.handle.net/10197/12050.

[5] S. Hu, D. Chen, and T. Mo, "A dual-band frequency tunable complex filter with stable quality-factor in different temperatures," in *2015 IEEE 11th International Conference on ASIC (ASICON)*, 2015, pp. 1–4.
[6] M. Tohidian, I. Madadi, and R. B. Staszewski, "3.8 A Fully Integrated Highly Reconfigurable Discrete-Time Superheterodyne Receiver," in *2014 IEEE International Solid-State Circuits Conference Digest of Technical Papers (ISSCC)*, 2014, pp. 1–3.
[7] M. Tamura, H. Takano, S. Shinke, H. Fujita, H. Nakahara, N. Suzuki, Y. Nakada, Y. Shinohe, S. Etou, T. Fujiwara, and Y. Katayama, "30.5 A 0.5V BLE Transceiver with a 1.9mW RX Achieving −96.4dBm Sensitivity and 4.1dB Adjacent Channel Rejection at 1MHz Offset in 22nm FDSOI," in *2020 IEEE International Solid- State Circuits Conference - (ISSCC)*, 2020, pp. 468–470.
[8] B. J. Thijssen, E. A. M. Klumperink, P. Quinlan, and B. Nauta, "30.4 A 370μW 5.5dB-NF BLE/BT5.0/IEEE 802.15.4-Compliant Receiver with >63dB Adjacent Channel Rejection at >2 Channels Offset in 22nm FDSOI," in *2020 IEEE International Solid- State Circuits Conference - (ISSCC)*, 2020, pp. 466–468.
[9] R. B. Staszewski, D. Leipold, and P. T. Balsara, "Direct frequency modulation of an ADPLL for bluetooth/GSM with injection pulling elimination," *IEEE Transactions on Circuits and Systems II: Express Briefs*, vol. 52, no. 6, pp. 339–343, 2005.

Suoping Hu (S'16–M'21) was born in Changzhou, China. He received the B.E. degree in integrated circuit design and system from Tianjin University (TJU), Tianjin, China, in 2013, and the M.Sc. degree (Hons.) in electronic science and technology from Shanghai Jiao Tong University (SJTU), Shanghai, China, in 2016. Afterwards, he joined University College Dublin (UCD), Dublin, Ireland, as a PhD student. He successfully defended his PhD defense in January 2021. Since 2017, he has been leading a joint research project with Analog Devices, Cork, Ireland, on a ULP Receiver.

In 2018, he was an IC Design Intern with Qualcomm, Cambridge, U.K., where he was with the RFIC Design Group for three months. His current research interests include ultra-low-power receivers, analog and radio frequency circuits.

Dr. Hu serves as a Reviewer for the IEEE JOURNAL OF SOLID-STATE CIRCUITS and the IEEE TRANSACTIONS ON CIRCUITS AND SYSTEMS—II: EXPRESS BRIEFS.

Peng Chen (S'15–M'20) received his B.Sc. degree in Electronics from Huazhong University of Science and Technology, Wuhan, China, and M.Sc. in Microelectronic from TU Delft, Delft, the Netherlands, in 2012 and 2014 respectively (MSc thesis done at IMEC Holst Center in Eindhoven, NL). He received his Ph.D. degree in 2019 from University College Dublin.

From 2014 to 2015, he worked as a test manager for Huawei Technologies in Amsterdam. From 2017 to 2018, he was a visiting research assistant in University of Macau. From 2019 to 2021, he was with Lund University as a post-doctoral researcher. He is now with the Wuxi Grandmicro, China. His research interests include time domain data converters, frequency synthesizers and wideband receiver.

Philip Quinlan obtained a B.Eng. in Electronic Engineering and an M.Eng. in Computer Science from the University of Limerick in 1983 and 1994 respectively. From 1983-1998 he worked in Analog Devices, Limerick, Ireland on the design of mixed-signal CMOS products for Hard Disk-Drive (HDD) Servo and Read Channels. In 1998 he joined ST Microelectronics, Longmont, Colorado, USA where he worked on the development of PRML Read-Channel technology. In 2001, he joined Analog Devices, Cork, Ireland, where he led a design team on the development of a family of high-performance, low-power Transceiver products. Since 2015 he has been a Technology Director at Analog Devices, working on the development of advanced ultra-low-power Radio Technologies. His interests include the design of low-power analog CMOS circuits and signal-processing techniques employed in Wireless Digital Communication Channels. He has authored or co-authored 15 technical journal and conference papers and holds 16 granted US patents.

Robert Bogdan Staszewski (M'97–SM'05–F'09) was born in Bialystok, Poland. He received the B.Sc. (*summa cum laude*), M.Sc., and Ph.D. degrees in electrical engineering from the University of Texas at Dallas, Richardson, TX, USA, in 1991, 1992, and 2002, respectively. From 1991 to 1995, he was with Alcatel Network Systems in Richardson, TX, USA, involved in SONET cross-connect systems for fiber optics communications. He joined Texas Instruments Incorporated, Dallas, TX, USA, in 1995 where he was elected Distinguished Member of Technical Staff (limited to 2% of technical staff). From 1995 to 1999, he was engaged in advanced CMOS read channel development for hard disk drives. In 1999, he co-started the Digital RF Processor (DRP) group within Texas Instruments with a mission to invent new digitally intensive approaches to traditional RF functions for integrated radios in deeply-scaled CMOS technology. He was appointed as a CTO of the DRP group from 2007 to 2009. In 2009, he joined the Delft University of Technology, Delft, The Netherlands, where currently he holds a guest appointment of Full Professor (*Antoni van Leeuwenhoek Hoogleraar*). Since 2014, he has been a Full Professor with the University College Dublin (UCD), Dublin, Ireland. He is also a Co-Founder of a startup company, Equal1 Labs, with design centers located in Silicon Valley and Dublin, Ireland, aiming to produce single-chip CMOS quantum computers. He has authored or co-authored five books, seven book chapters, 130 journal and 200 conference publications, and holds 200 issued US patents. His research interests include nanoscale CMOS architectures and circuits for frequency synthesizers, transmitters and receivers, as well as quantum computers.

Prof. Staszewski was a TPC Chair of 2019 ESSCIRC in Krakow, Poland. He was a recipient of the 2012 IEEE Circuits and Systems Industrial Pioneer Award. In May 2019, he received the title of Professor from the President of the Republic of Poland.